Transposition from a batch to a continuous process for microencapsulation by interfacial polycondensation

Félicie Theron, Zoé Anxionnaz-Minvielle, Nathalie Le Sauze, Michel Cabassud

Transposition from a batch to a continuous process for microencapsulation by interfacial polycondensation

Félicie Theron[a,b,*], Zoé Anxionnaz-Minvielle[c], Nathalie Le Sauze[a,b], Michel Cabassud[a,b]

[a] Université de Toulouse; INPT, UPS; Laboratoire de Génie Chimique; 4 Allée Emile Monso, BP 84234, F-31432 Toulouse, France
[b] CNRS; Laboratoire de Génie Chimique; F-31432 Toulouse, France
[c] CEA LITEN, Alternative Energies and Atomic Energy Commission,17 rue des Martyrs, 38054 Grenoble Cedex 9, France

Keywords:
Microencapsulation
Interfacial polycondensation
Continuous process
Static mixer
Milli reactor
Coiled tube reactor

A B S T R A C T

A novel continuous process is proposed and investigated to produce microcapsules by interfacial polycondensation. Polymeric microcapsules are obtained via a two-step process including an initial emulsification of two immiscible fluids in static mixers and a subsequent interfacial polycondensation reaction performed in two different continuous reactors, the Deanhex heat exchanger/reactor or a classical coiled-tube. This study is carried out through a step by step approach. A model system involving polyurea as the polymeric membrane and cyclohexane as the encapsulated species is chosen. A semi-batch reaction kinetic study is first performed in order to obtain kinetics data of the polycondensation reaction and to highlight hydrodynamic issues that can happen when running the encapsulation reaction in classical stirred tank. Parameters influencing droplets size obtained when carrying out emulsification in static mixers are then investigated. The hydrodynamic of the Deanhex reactor used is also characterized in terms of mixing time and residence time distribution. To validate the innovative continuous process, the emulsion droplets obtained at the static mixer outlet are encapsulated firstly in the Deanhex reactor and secondly in the coiled-tube. The apparent reaction kinetics and microcapsules characteristics corresponding to different operating conditions are discussed.

1. Introduction

Microencapsulation is a widely used method to produce microparticles enclosing an active ingredient. These microparticles may be either solid networks forming matrices in which is dispersed the solid or liquid active substance called microspheres, or core–shell systems made of a solid wall enclosing and protecting a liquid or solid core called microcapsules [1–3]. The present study concerns the synthesis of the last form of microparticles. In general, the size of microcapsules ranges from 5 to 200 μm [4]. Interest for microencapsulation is related to the development of various applications such as carbonless copying paper with capsules diameters from several micrometers to 30 μm, medicines, flavor in the food industry [5,6], and cosmetics. Since several years, microencapsulation is also used by the textile industry [7] to propose fragranced or active clothes to customers like perfumed tissue papers or slimming tights.

Microcapsules are high added value products with many different properties which are not easily controllable. These properties may be adjusted and optimized during the formulation step. A homogeneous production without any discrepancy towards the expected properties must be guaranteed by the manufacturing process.

The present work aims at demonstrating the design and the feasibility of a continuous process of microencapsulation by interfacial polycondensation. This chemical encapsulation technique consists in a reaction between two reactive monomers at the interface of droplets. An emulsion involving the active ingredient and a first monomer inside droplets is firstly prepared, then a second monomer is added in the continuous phase. The interfacial reaction at droplets interface starts as soon as both monomers are in contact. Polymer walls prepared by interfacial polycondensation may be for example polyester, polyamide, polyurethane, or polyurea [4]. Continuous processes are well adapted to interfacial polycondensation that present relatively fast reaction kinetics.

Nowadays batch processes involve high volume reactors. They are reliable and flexible, their operating modes are well-known and residence times in such processes are as long as required. Moreover both steps involved in the process require different hydrodynamic conditions that are hardly compatible in the same apparatus. The final microcapsules size distribution is fixed during the

* Corresponding author at: Université de Toulouse; INPT, UPS; Laboratoire de Génie Chimique; 4 Allée Emile Monso, BP 84234, F-31432 Toulouse, France.
Tel.: +33 534323672.
E-mail address: felicie.theron@mines-nantes.fr (F. Theron).

doi:10.1016/j.cep.2012.01.001

emulsification step that requires high shear conditions. Then it is important to insure that no coalescence occurs before adding the second monomer and that no agglomeration phenomenon happens during the polycondensation reaction. Concerning this reactive step the key parameters are the hydrodynamic conditions and the second monomer addition rate [8–10]. The continuous phase monomer must be quickly homogenized in this phase in order to guarantee that the reaction takes place simultaneously at the interface of all droplets so as to insure a good homogeneity of microcapsules properties, what requires a fast mixing time. Moreover the flow conditions in the reactor must tend to a plug flow in order to avoid the agglomeration phenomenon and to insure good membrane thickness homogeneity.

That is the reason why the present paper proposes to use continuous technologies well adapted to the hydrodynamic issues of both successive steps involved in interfacial polycondensation. This approach allows to remove hydrodynamic barriers previously cited, while keeping the emulsion droplets size distribution during the polycondensation reaction. In order to increase the process yield we wish to increase as much as possible the microcapsules concentration during the reaction without any agglomeration phenomenon.

In this study the emulsification step is performed in a Sulzer SMX^{TM} static mixer and the reactive step in a wavy channel (Deanhex reactor) or in a classical coiled-tube reactor. Static mixers are fixed structures inserted into cylindrical pipes. The Sulzer SMX mixer consists in an array of crossed bars arranged at an angle of 45° against the tube axis. Static mixers offer the advantages to represent low investments and energy costs compared to a classical stirred tank [11]. Liquid–liquid dispersion or emulsification is achieved by flowing the two immiscible liquids co-currently through the mixer. The energy cost of the operation is related to the pumps required to transport the liquids through the mixer. The energy consumption can be estimated through pressure drop measurements and enables to predict the droplets size [11–15]. Static mixers are particularly interesting for liquid–liquid dispersion as shear stress is more uniform than in stirred tanks, what results in lower times needed to reach the equilibrium between break up and coalescence [16,17].

The Deanhex reactor is an example of heat exchanger/reactor which technology is based on the plate heat exchangers [18]. By combining a heat exchanger and a reactor in the same apparatus, an accurate thermal control of the reaction is expected. Moreover the reactors require a sufficient residence time to complete the chemical syntheses. Thus, a way to intensify heat and mass transfers while operating in laminar flow is to structure the chemical path [19–21]. This is the main characteristic of the Deanhex reactor which is made of a reaction plate inserted between two cooling plates. A wavy milli-channel has been machined in the first one. The thermo-hydraulic characterizations of this 2D geometry have been made in homogeneous liquid phase [22]. It shows narrow residence time distributions, high heat and mass transfers and moderate pressure drops in transitional flow regime (Reynolds number around 2000).

The helically coiled tube reactor is well documented in the literature [23–26]. In such reactors the action of centrifugal force on fluid elements moving with different axial velocities in a curved circular pipe induces a secondary flow in the tube cross-section plane. This secondary flow field leads to increased pressure drops, but also to higher heat and mass transfer coefficients, and to narrowed residence times.

The continuous encapsulation process investigated is tested with a model system described in the literature and already studied in batch processes [27–31]. The reaction involves hexamethylene diisocyanate (HMDI) and hexamethylene diamine (HMDA). The emulsification step involves cyclohexane containing HMDI (first monomer) as the dispersed phase, and water as continuous phase. This emulsion is stabilized using a surfactant: Tween 80. Continuous phase (water + Tween 80) containing HMDA as second monomer is then added to the emulsion to initiate the reactive step. The emulsion is thus diluted. The two monomers react through an athermal reaction to form a polyurea membrane at the droplets interface:

$$nH_2N{-}(CH_2)_6{-}NH_2 + nO{=}C{=}N{-}(CH_2)_6{-}N{=}C{=}O \rightarrow -[HN{-}(CH_2)_6{-}NH{-}OCNH{-}(CH_2)_6\,NHCO]n-$$

$$\text{HMDA} + \text{HMDI} \rightarrow \text{Polyurea}$$

The methodology used to transfer the batch encapsulation process to a continuous one involves several experimental steps presented in Fig. 1. The first part of this paper reports the preliminary studies performed in order to acquire the experimental data required to set up the continuous process. The encapsulation reaction is first investigated through a semi-batch process in order to collect kinetics data and to highlight hydrodynamic issues presented by the classical stirred tank. Emulsification in SMX static

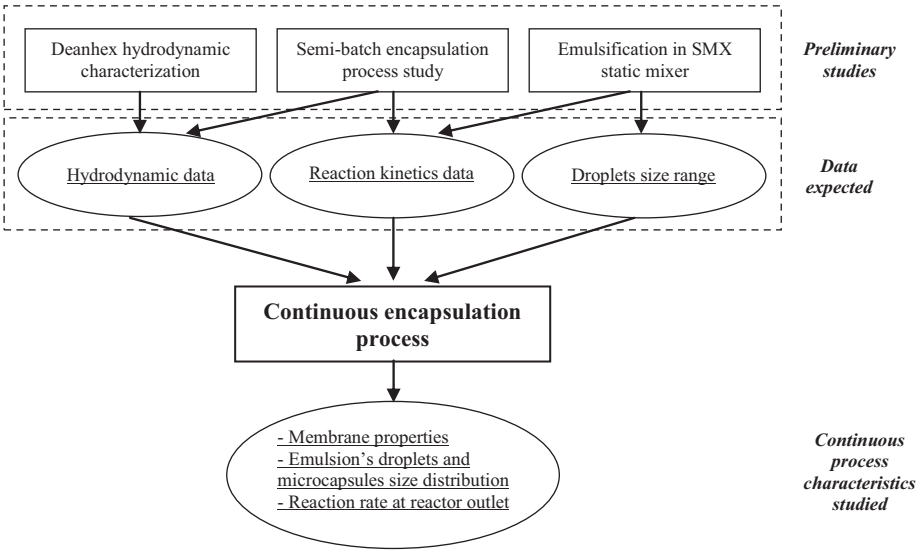

Fig. 1. Schematic diagram of the methodology used to transfer the batch encapsulation process to a continuous one.

Table 1
Physico-chemical properties of continuous and dispersed phases involved in the present study.

Fluid	Water – Tween80 (1.5 vol.%)	Cyclohexane
Density (kg m^{-3})	995	770
Viscosity (Pa s)	0.0010	0.0009

Fig. 2. A set of 10 SMX elements.

mixer is studied in order to evaluate the influence of hydrodynamic parameters on droplets sizes. The Deanhex reactor is characterized in terms of hydrodynamic performances.

The second part of this paper deals with the investigations of the continuous process proposed. This process is first assessed through membrane properties, apparent reaction kinetics, and microcapsules size distribution. The influence of the reaction temperature on both reaction kinetics and microcapsules size distribution is also analyzed. Finally the continuous process is carried out without surfactant in the continuous phase.

2. Experimental

2.1. Materials

HMDA and HMDI used as monomers are purchased from Acros Organics. The surfactant and oil phase are respectively Tween 80 and cyclohexane, and are purchased from Panreac and Acros Organics. Viscosities of continuous and dispersed phases are measured using an AR2000 rheometer (AR instruments). Monomers are added in such low concentration in both phases that viscosities and densities can be considered as those of the pure aqueous and oil phases, as detailed in Table 1.

The interfacial tension between both phases at equilibrium is measured using the Whilelmy plate method with a Balance 3S (GBX Instruments tensiometer). It is equal to 3.5 mN m^{-1} and it is not modified by monomers.

2.2. Experimental set up and procedure

The emulsification step is performed in a stainless steel tube packed with a stainless steel Sulzer SMX static mixer made of 10 elements (see Fig. 2). The diameter of each element D, the aspect ratio D/L (element diameter/element length), the porosity ε, the hydraulic diameter D_h, and the crossbars thickness δ are given in Table 2.

The reactive step is carried out either in a Deanhex reactor either in a classical coiled-tube reactor. The Deanhex reactor is made of three plates: a cooling (or heating) plate called 'utility plate' sandwiched between a closing plate and a 'process plate' in which flow the reactants. The 'utility plate', made of aluminium, is removed for the implementation of the interfacial polycondensation reaction due to its athermal aspect. The 'closing' and 'process' plates are made of polymethylmethacrylate (PMMA) which is transparent in order to visualize the flow during the experiments (see

Table 2
Geometrical data of the SMX mixer.

D (mm)	D/L	ε	D_h (mm)	δ (mm)
10	1	0.67	2.45	0.99

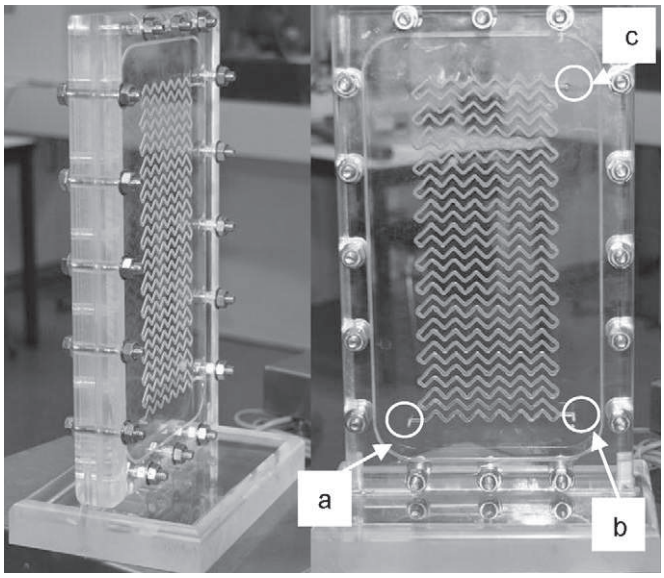

Fig. 3. Deanhex reactor: (a) primary inlet; (b) secondary inlet; (c) outlet.

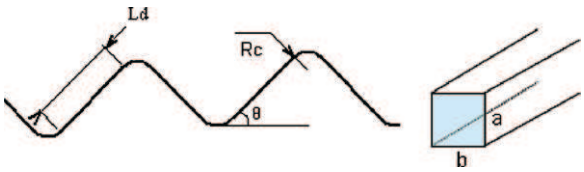

Fig. 4. Schematic view of the geometrical parameters of the Deanhex reactor channel.

Table 3
Geometrical data of the corrugation parameters of the Deanhex reactive channel.

	d_h (mm)	a/b	R_c/d_h	L_d (mm)	θ (°)	L_{tot} (mm)
Deanhex 2 × 2	2	1	2	20.28	90	3400
Deanhex 4 × 4	4	1	1	20.28	90	3400

Fig. 3). The square cross section wavy channel is machined on the 'process plate' and two geometries are tested in this study. They are characterized by the hydraulic diameter, d_h, the aspect ratio, a/b (channel height/channel width), the curvature ratio, R_c/d_h, the straight length between two bends, L_d, the angle of the bend, θ and the total developed length of the channel, L_{tot}. These parameters are represented in Fig. 4 and the geometrical data are given in Table 3.

The Deanhex reactor has two flow inlets in order to mix the two reactants in the wavy channel and avoid a limiting upstream premix. Two temperature and pressure probes are set up at the inlet and the outlet of the reactor.

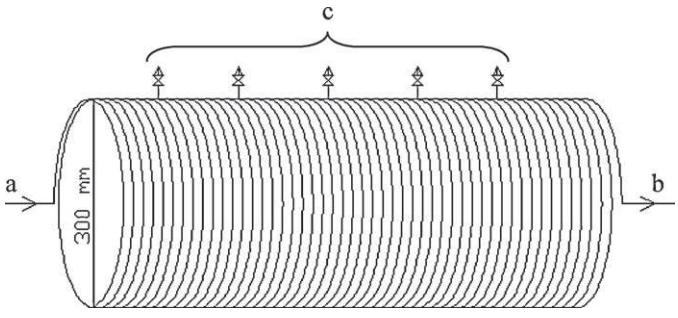

Fig. 5. Coiled-tube reactor: (a) inlet; (b) outlet; (c) sampling valves.

The coiled-tube reactor (cf. Fig. 5) consists in a 4 mm inner diameter 50 m length pipe, with a coil diameter of 300 mm. Five sampling valves are set up along the pipe.

Fig. 6 presents a schematic diagram of the experimental set up. During each experiment the emulsion flows through the static mixer where the flow rate is fixed to 167 L h^{-1}. The dispersed phase concentration $\Phi_{emulsion}$ is fixed thanks to respective continuous and dispersed phase volumes. The largest part of the emulsion flow recirculates through a tank, whereas a small fraction of this stream flows through the reactor. The emulsion flow rate passing through the reactor is determined by weighing the volume collected at the reactor outlet for a given experimental time. The microcapsules concentration $\Phi_{microcapsules}$ is controled by choosing the relevant ratio of both the emulsion and the continuous phase containing HMDA flow rates:

$$\phi_{microcapsules} = \frac{\phi_{emulsion} Q_{emulsion}}{Q_{tot}} \quad (1)$$

where $\Phi_{emulsion}$ is the dispersed phase concentration in the emulsion, and Q_{tot} is the total flowrate in the reactor.

The pH of the slurry's continuous phase at the reactor outlet is measured with a PHM210 Meterlab pH-meter (radiometer analytical) in order to calculate the HMDA conversion. The pH is given with a 0.01 pH unit precision.

Finally samples of emulsion droplets at the static mixer outlet and microcapsules at the reactor outlet are collected in order to characterize their size distributions and to analyze microcapsules properties.

2.3. Droplets and microcapsules characterization

Some microcapsules properties are analyzed in order to validate the continuous process. The determination of both emulsion droplets and microcapsules size distributions allows to evaluate whether the dispersed phase size distribution is kept constant during the polycondensation reaction. Thermal properties of the polymeric membrane and its chemical structure are identified using respectively differential scanning calorimetry and Fourier Transformed Infra-Red spectroscopy.

2.3.1. Droplets and microcapsules size distribution

Size distributions of both emulsion droplets and microcapsules are determined using a Mastersizer 2000 (Malvern Instruments).

2.3.2. Differential scanning calorimetry (DSC)

Thermal properties of the polymeric membrane are analyzed via differential scanning calorimetry (DSC) with a Q2000 calorimeter (TA Instruments). Before analysis, the microcapsules are recovered from the slurry by filtration, washed with ethanol to remove unreacted monomers from the surface, filtered again, and dried in a vacuum oven at 25 °C for at least 24 h. Samples about 2 mg are sealed in DSC pans and heated from 25 °C to 400 °C at a heating rate of 10 °C min^{-1}.

2.3.3. Fourier Transformed Infra-Red spectroscopy (FTIR)

Infrared spectra of the polymeric membrane are obtained with a Nicolet 5700 (Thermo Fischer) spectrophotometer. Before each analysis the membrane samples are treated as for DSC measurements.

3. Preliminary studies

3.1. Reaction kinetics study in semi-batch conditions

In the batch to continuous transposition approach performed, a semi-batch reaction study is carried out before performing the whole process continuously. The emulsion is generated in the SMX static mixer and the reaction runs in a classical stirred tank. It is obvious that reaction characteristic times must be determined to design continuous reactors. Moreover batch studies enable to highlight typical issues occurring in stirred tank hydrodynamic conditions and that may be avoided when working continuously.

The semi-batch study is described in this section. The experimental method chosen to follow the reaction kinetics is first detailed. Then typical kinetics results are shown. And finally some hydrodynamic issues encountered in classical stirred tanks are exhibited.

The reaction is performed in a 4 baffles jacketed 1 L tank, stirred with a 3 blades turbine. The stirring speed is fixed to 200 rpm, corresponding to the minimum speed to keep the suspension homogeneous. The reactor is also equipped with a pH-sensor (Mettler–Toledo) connected to a computer in order to acquire continuous phase pH profiles.

Before experiments the tank is poured with the HMDA solution, the stirring speed as well as the jacket temperature is fixed, and the pH-acquisition is started. Then the respective flowrates of both water and cyclohexane-HMDI solution in the static mixer are fixed. During this transient time of flowrates adjustment the emulsion at mixer outlet is conveyed to a receiving tank. As soon as the targeted total flowrate and dispersed phase concentration are reached the fixed volume of emulsion flowing at static mixer outlet is poured into the tank.

3.1.1. Experimental measurement of reaction kinetics

The experimental acquisition of kinetics data of interfacial polycondensation reactions is rather difficult due to their inhomogeneity and fast kinetic rates. The most often studied parameters are the membrane thickness or the continuous phase monomer consumption versus time. The membrane thickness measurement has been used by several authors [32–35].

But this method is especially difficult to carry out because of the low membranes thickness and the experimental barriers such as reaction quenching, sample preparation and representativeness.

For the case of polyurea membranes, the continuous phase monomer is an amine that confers a basic character to the aqueous solution. The continuous phase pH recording thus enables to determine the amine concentration profile as a function of time. This technique has been used by Yadav et al. [27,36], Kubo et al. [37], Dhumal et al. [29] and Wagh et al. [31] and is chosen in this paper.

The transposition from the continuous phase pH profile to the amine (here HMDA) concentration requires a calibration step. It consists in measuring pH of aqueous solutions with various known HMDA concentrations. This calibration is carried out here in presence of surfactant in the continuous phase and with dispersed phase droplets in order to reproduce experimental conditions during encapsulation reactions. It is performed at 25 °C. The calibration curves corresponding to the pH with and without dispersed phase droplets are presented in Fig. 7. The HMDA concentration ranges from 10^{-2} to 2×10^{-4} mol L^{-1} which corresponds to pH ranging from 11.47 to 9.96.

The pH of the continuous phase is slightly lower when cyclohexane droplets are involved. But the discrepancy is always lower than 2%. In the HMDA concentration range studied the relationship between the pH and the HMDA concentration is linear in log-normal representation. This relationship can thus be modelled, in the HMDA concentration range considered, as follows:

$$C_{HMDA} = 1.7 \times 10^{-15} \times C_h^{-1.1} \quad (2)$$

where C_{HMDA} and C_h are the HMDA and the hydrogen ions concentrations in the continuous phase. The constant as well as the

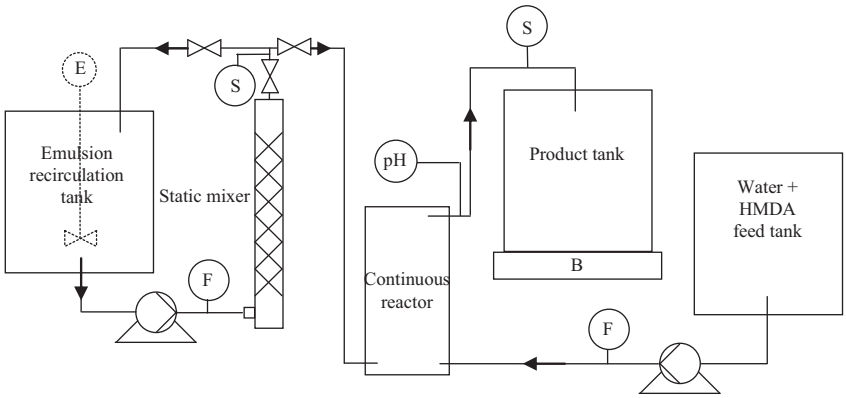

Fig. 6. Schematic diagram of the experimental set up: F: flowmeter; B: balance; E: engine; S: sampling.

C_h exponent have been determined in order to fit with calibration points.

From pH profiles recorded during encapsulation reactions it is possible to determine the HMDA conversion X_{HMDA} evolution through the following equation:

$$X_{HMDA} = \frac{C_{HMDA,0} - C_{HMDA}}{C_{HMDA,0}} = 1 - \left(\frac{C_h}{C_{h0}}\right)^{-p} = 1 - 10^{(pH_0 - pH)p} \quad (3)$$

where $C_{HMDA,0}$ and $C_{h,0}$ are the initial HMDA and hydrogen ions concentrations in the continuous phase, pH_0 is the initial pH value, and p is equal to 1.1.

According to the calibration pH range (11.47–9.96) the HMDA conversion can be quantified up to 0.98–0.95 for initial HMDA concentration ranging from 7.7×10^{-3} to 2.9×10^{-3} mol L^{-1}.

3.1.2. Reaction kinetic results

The characteristic time chosen in this work is the t_{95} defined as the time required to reach a HMDA conversion of 95% which is the maximum conversion value measurable according to the calibration curve (cf. Fig. 7).

Fig. 8 shows the HMDA conversion evolution versus time calculated from Eq. (3). t_{95} is found to be 39 s for the experimental conditions tested which is low enough to perform the reaction in a continuous reactor.

A reproducibility study has shown that the discrepancy is always lower than 2% before reaching 95% conversion.

3.1.3. Hydrodynamic issues of encapsulation reaction in classical stirred tank

The use of static mixers to generate the emulsion for cases of two-steps processes enables to generate fast well-controlled droplets size distributions. It is thus a real improvement compared to entire batch processes. For example, such a semi-batch process has been investigated successfully by Hirech et al. [38] to perform microencapsulation of an insecticide by interfacial polycondensation.

In this study two different microcapsules concentrations, 5% and 10% in volume, are tested. When working with 5% in volume of microcapsules, no evolution of the dispersed phase size distribution is observed. When increasing the microcapsules concentration to 10% in volume, Fig. 9 shows the obtained results. These results are the emulsion droplets size distribution and three microcapsules size distributions at different reaction times. The apparition of a second peak at largest sizes that becomes more and more important during microencapsulation points out an aggregation phenomenon.

The assumption of a droplets coalescence phenomenon during the transport from the static mixer to the tank may be rejected as the major peak of the distribution in the first time of the reaction (t = 28 s) is almost confounded with the emulsion droplets size distribution. The microcapsules size distribution evolution may be explained by an irreversible agglomeration phenomenon that takes place in the tank, and which becomes particularly important as conversion rate increases (at t = 28 s the HMDA conversion is already of 90%), and thus pH decreases.

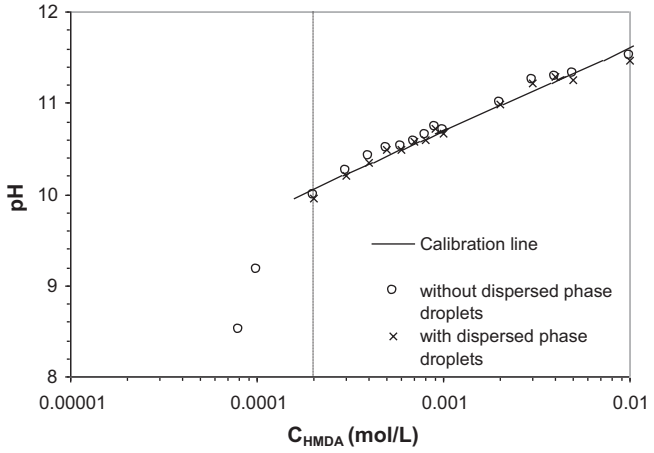

Fig. 7. Calibration curves representing continuous phase pH as a function of HMDA concentration with and without dispersed phase droplets.

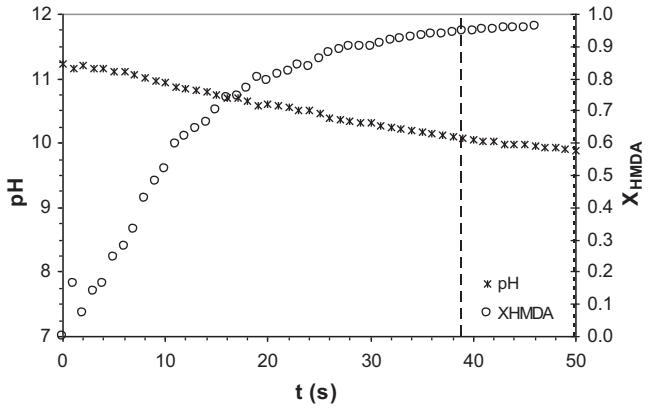

Fig. 8. Time evolution of both continuous phase pH and resulting HMDA conversion for a batch reactor experiment with T = 25 °C, $C_{HMDA,0} = 4.1 \times 10^{-3}$ mol L^{-1}, and $\Phi_{microcapsules} = 0.05$.

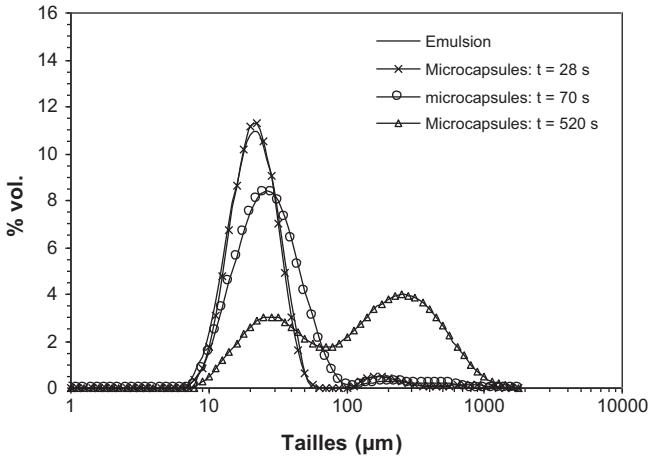

Fig. 9. Comparison between emulsion droplets and microcapsules size distribution with $T = 25\,^{\circ}C$, $C_{HMDA,0} = 7.7 \times 10^{-3}$ mol L^{-1}, and $\Phi_{microcapsules} = 0.10$.

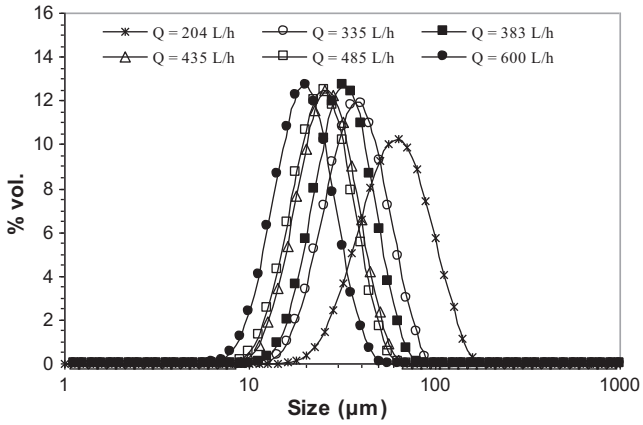

Fig. 10. Influence of the total flowrate on droplet size distribution for experiments with $n_e = 10$ and $\Phi_{emulsion} = 0.25$.

The agglomeration phenomenon may be due to a too high agitation speed as suggested in the literature [8,10]. In fact, increasing the stirring speed results in increasing the probability of microcapsules collisions, which can promote a sticking phenomenon between microcapsules. Thus a way to avoid this phenomenon is to propose a reactor with appropriate hydrodynamic conditions.

3.2. Emulsification in SMX static mixer

The emulsification step enables to fix the future microcapsules size distribution. That is why the influence of the different parameters influencing this operation must be precisely identified and controlled. Emulsification in the SMX static mixer has been previously studied for the system used [11]. This mixer has been chosen as it allows obtaining narrow droplet size distributions. The influence of different parameters like the number of mixing elements (i.e. mixer length) and the total flowrate on the mean droplets size distribution has been highlighted for a fixed dispersed phase concentration of 25% in volume.

3.2.1. Influence of the total flowrate

For a flowrate range of 200–600 L h^{-1}, droplet size distributions in volume obey to a log-normal function as shown in Fig. 11. Size distributions are characterized in terms of Sauter mean diameter D_{32} that are equals to 20 to 60 µm (cf. Table 4) for distributions presented in Fig. 10. Such sizes are relevant for many applications like insecticide for example [38].

3.2.2. Influence of the number of elements

For one pass through the mixer it appears that the break up phenomenon mostly occurs in the first 5 mixer elements [11]. From 5 to 20 elements, the mean diameter does not decrease significantly even though no constant diameter is reached. The mean energy dissipation rate in the mixer that rules the energy cost of the operation is proportional to the number of mixing elements. That is why ten mixing elements are chosen in order to make a compromise between the mean droplet size and the energy cost.

The adsorption kinetics of the surfactant at droplets interface is very low compared to the time of one pass through the mixer. In the process studied the emulsion recirculates in the mixer, so the evolution of the surfactant adsorption phenomenon with time enables to carry out experiments at a total flowrate (167 L h^{-1}) lower than those presented in Fig. 10 and to reach mean diameters of the same order.

Table 4
Values of Sauter mean diameter D_{32} as a function of Q corresponding to the droplets size distributions presented in Fig. 11.

Q (L h^{-1})	204	335	383	435	485	600
D_{32} (µm)	58.1	36.8	31.8	25.6	24.3	19.4

3.3. Hydrodynamic study of Deanhex reactors

The coiled tube is also used to perform the interfacial polycondensation reaction. As it is well documented and studied in the literature [23–26], its hydrodynamic characterization is not presented.

Microencapsulation by interfacial polycondensation involves a fast and athermal reaction during which the size distribution of emulsion's droplets has to be maintained. Moreover the second monomer needs to be quickly homogenized in the continuous phase in order to ensure a homogeneous membrane thickness. Therefore, the main hydrodynamic characterizations concerning the RTD study and the evaluation of the mixing performances are summarized in this article.

Hydrodynamic characterization is an essential step before the implementation of a chemical reaction. For many fast kinetics reactions a narrow RTD will ensure high yields and selectivity without by-pass or stagnant zones. High mixing performances are important in case of fast chemical kinetics to avoid an inhomogeneous distribution of reactants and thus the local occurrence of secondary reactions. Pressure drop is directly linked to the operating costs and a high thermal transfer will allow an accurate control of the operating temperature (close to isothermal conditions). The Deanhex reactor has already been characterized in terms of residence time distribution (RTD), mixing performances, pressure drop and thermal transfer in the case of monophasic flow [39].

3.3.1. RTD measurements

The RTD measurement method involves a spectro-photometric technique that entails a colored tracer: $KMnO_4$. Two measuring probes are set up at the reactor inlet and outlet. They registered the $KMnO_4$ absorbance versus time. This allows to plot the tracer concentration and thus the RTD profiles vs time at the reactor inlet and outlet. The acquisition time is set to 0.12 s and each experiment is performed at room temperature. The experimental RTD is modeled by a N tanks in series model [40]. This means that the reaction channel will be equivalent to N tanks in series which total volume is equal to the channel volume. $N = 1$ corresponds to the perfectly mixed continuous reactor whereas $N = \infty$ corresponds to the perfect plug flow reactor. Thus, the higher N the more the flow behaves

Table 5
Operating conditions and results of the RTD experiments.

	Flow rate ($kg\,s^{-1}$)	Reynolds number	N_{tank}/L
Deanhex 2 × 2	5.0	697	42
	8.0	1111	44
	12.0	1667	59
	15.0	2086	64
Deanhex 4 × 4	9.0	627	49
	12.0	835	54
	15.0	1040	67
	18.1	1254	108
	21.8	1514	108
	24.5	1701	130

like a plug flow, which is necessary to perform safely and efficiently chemical syntheses.

The operating conditions (flow rates and Reynolds number) and the results in terms of equivalent number of stirred tanks per length unit (N_{tank}/L) are given in Table 5. N_{tank} is the number of tanks modeling the channel RTD and L is the channel length.

The RTD characterization shows that in the Reynolds range of 700–2000 the flow behaves like a quasi-perfect plug flow, what is provided by the wavy design of the channel ($N > 40$). Each bend actually generates a secondary flow in the form of counter-rotating symmetrical vortices in the duct cross section [41]. This promotes the homogenization of the flow temperature, concentration and momentum downstream the bends and thus reduces the axial dispersion within the flow. Similar results are observed in both Deanhex 2 × 2 and Deanhex 4 × 4.

As illustrated in Fig. 11, no dead zones or by-pass are observed which is necessary to guarantee a homogeneous microcapsules membrane thickness at the reactor outlet.

3.3.2. Mixing performances

In order to characterize the global mixing level of each reactor, the reaction of discoloration of an iodine solution with sodium thiosulfate is implemented according to the following reaction scheme:

$$I_2(\text{brown}) + 2Na_2S_2O_3(\text{colorless}) \rightarrow 2NaI(colorless) + Na_2S_4O_6(\text{colorless})$$

This homogeneous reaction is instantaneous and mixing limited. As a consequence, at steady state, by measuring the required length to complete the discoloring of iodine, the mixing time can be easily determined. Thiosulfate concentration is equal to $1.4 \times 10^{-2}\,mol\,L^{-1}$ and the iodine one is $5 \times 10^{-3}\,mol\,L^{-1}$. The flowrates ratio is equal to 1 in each geometry.

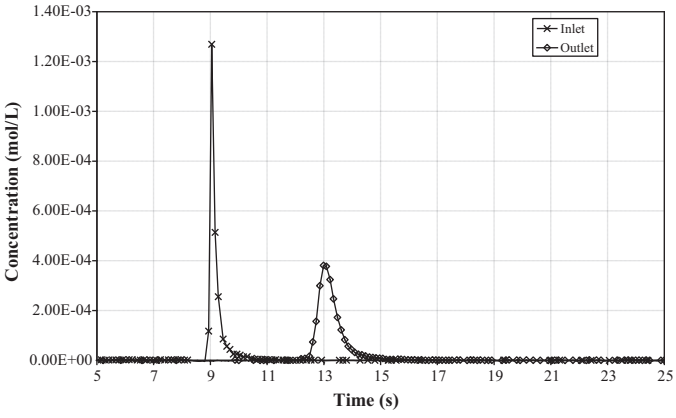

Fig. 11. Residence time distribution in Deanhex 2 × 2 ($Q = 15.0\,L\,h^{-1} - N_{tanks} = 218$).

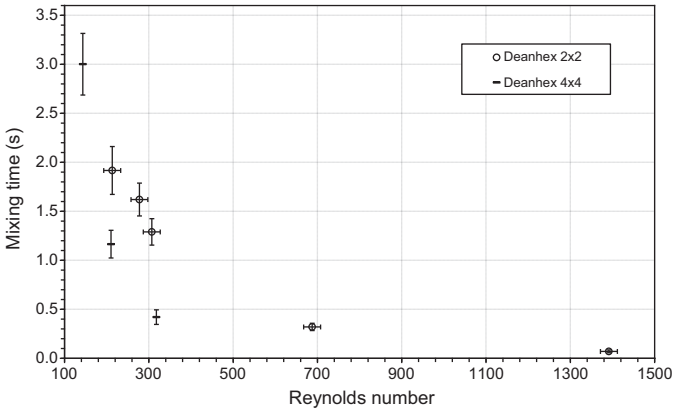

Fig. 12. Mixing time versus Reynolds number.

As expected (cf. Fig. 12), mixing times rapidly decrease when the Reynolds number increases. The influence of the channel geometry is real for low Reynolds number ($Re < 700$). Above this value, the mixing times tend to be equal and quite short ($t_m < 0.2$ s) compared to the period during which the apparent kinetics is controlled by the chemical reaction, i.e. several ten seconds.

Therefore, the polycondensation reaction is implemented at Reynolds number higher than 600. The short mixing time ($t_m < 0.2$ s) in the Deanhex reactor may enable to decrease the time needed to homogenize the second monomer in continuous phase and thus to ensure a better membrane thickness homogeneity.

4. Results and discussion

4.1. Experimental conditions

Experiments are conducted in order to evaluate the influence of working parameters on the microcapsules characteristics and apparent reaction kinetics. The parameters under study are the microcapsules concentration, the temperature, the HMDA initial concentration, the surfactant, and the type of reactor. Experimental conditions are detailed in Table 6. The total flow rate in the reactor Q_{tot}, the residence time t_r, the hydraulic Reynolds number Re_h and the temperature T characterize the flowing conditions through the three tested reactors, i.e. the coiled tube reactor and the two Deanhex reactors. For experiments in the coiled-tube the total flowrate is equal to the flowrate set up in Deanhex 4 × 4. In Table 6 two different dispersed phase concentrations appear: $\Phi_{emulsion}$ and $\Phi_{microcapsules}$ that are the dispersed phase concentrations respectively during the emulsification and the reactive step. σ is the interfacial tension between both phases involved in the emulsification step: cyclohexane containing HMDI and water containing Tween 80. When Tween 80 is not involved in the continuous phase the interfacial tension is of $47\,mN\,m^{-1}$ and is reduced to $3.5\,mN\,m^{-1}$ at equilibrium when the surfactant is used. The HMDA conversion X_{HMDA} at the reactor outlet appears in the last column of the table.

4.2. Polymer membrane properties

The membrane material chemical structure and microcapsules thermal properties are analyzed to check that the expected polymer is obtained. The following properties correspond to microcapsules obtained during experiment E1 involving the 2 mm width Deanhex, low capsule concentration of 5% in volume, and $T = 25\,°C$ (experiment E1).

Table 6
Experimental conditions for encapsulation experiments.

Exp. Ref.	Reactor	Q_{tot} ($L\,h^{-1}$)	t_r (s)	Re_h	$\Phi_{emulsion}$ (vol.%)	$\Phi_{microcapsules}$ (vol.%)	σ ($mN\,m^{-1}$)	T (°C)	$C_{HMDA,0}$ ($mol\,L^{-1}$)	X_{HMDA}
E1	Deanhex 2 × 2	5.0	9.6	686	25	4	3.5	25	4.1×10^{-3}	55
E2	Deanhex 2 × 2	4.9	9.7	673	25	10	3.5	25	7.7×10^{-3}	64
E3	Deanhex 2 × 2	5.2	9.4	714	25	11	3.5	32	7.7×10^{-3}	90
E4	Deanhex 4 × 4	9.9	19.4	680	25	10	3.5	25	7.7×10^{-3}	78
E5	Coiled tube	9.8	230	867	25	10	3.5	25	7.7×10^{-3}	93
E6	Coiled tube	10.0	226	884	25	6	47	25	4.7×10^{-3}	83

4.2.1. Microcapsules structure

Fig. 13 represents the FTIR spectra resulting from the analysis of the microcapsules shell material.

The FTIR spectra exhibits a strong band at about 3330 cm^{-1} that corresponds to hydrogen bonded N—H stretching vibration. C—H stretching vibrations of aliphatic diamine are detectable by bands at 2919 cm^{-1}, 2908 cm^{-1} and 1852 cm^{-1}. Moreover, the NCO peak of diisocyanates between 2275 cm^{-1} and 2242 cm^{-1} has disappeared due to the reaction between HMDI and HMDA. The hydrogen bonded urea carbonyl peak is observed at about 1623 cm^{-1}.

We can thus conclude that the reaction has been completed and that the wall polymer membrane formed is polyurea as expected.

4.2.2. Thermal properties

Depending on the use of the polymer, it is important to know its thermal properties like its melting point. That is why DSC analysis is realized on some shell material of microcapsules. Fig. 14 presents a thermogram of the polyurea material obtained.

This thermogram shows an endothermic peak at about 290 °C which corresponds to the melting point of the polyurea. On the thermogram also appear an endothermic peak at about 250 °C and an exothermic peak at about 252 °C. These results are in good agreement with Yadav et al. [36] thermograms resulting from DSC analysis of polyurea synthesized from the same monomers.

The first endothermic peak at about 250 °C corresponds to the melting of the imperfect crystals formed during the polymerization. The exothermic peak at about 252 °C probably results from a crystallization transition during which the polymer chains arrange themselves into the most ordered structure under the conditions of increased mobility. In order to assess the previous assumption, an additional DSC analysis is conducted. It consists in heating the polymer sample to a temperature slightly higher than the melting region (265 °C), cooling it to room temperature, and then heating it again through the same procedure as before. The result of this analysis shows neither the endothermic peak at 250 °C nor the exothermic one at 252 °C. This confirms that the peak at about 251 °C is due to a crystallization-transition.

Thus the DSC analysis enables to demonstrate that the polymer shell of microcapsules is a high-melting thermoplastic as expected.

From FTIR and DSC analysis of the polymer membrane we can conclude that the proposed continuous process enables to obtain the same polymer as the one synthesized through classical batch processes.

4.3. Continuous reaction kinetics aspects

4.3.1. HMDA conversion at the Deanhex reactor outlet

The pH is measured at reactor outlet and HMDA conversion is calculated from the measured value according to the expression (3) (cf. Section 3).

The conversion at the Deanhex 2 × 2 outlet (experiment E1) is compared to batch data at the same reaction time for similar experimental conditions in Fig. 15.

The amine conversion at reactor outlet is 55% whereas it is 65% at the same time in batch conditions.

This 15% deviation may be explained by the uncertainty of pH measurement at reactor outlet. One can thus consider that the apparent reaction kinetics is not modified when using the Deanhex reactor.

The mixing time in the Deanhex used is about 0.2 s whereas it is about 10 s in semi-batch conditions. The comparison between results obtained in both cases shows that the reaction apparent kinetics is not accelerated when the HMDA homogenization time in the continuous phase decreases. This confirms that the HMDA diffusion in the continuous phase is not a limiting phenomenon and that the apparent reaction kinetics is only controlled by the chemical reaction in the HMDA range investigated ($X_{HMDA} \leq 95$).

When increasing the microcapsules concentration from 5% to 10% in volume (experiment E2) the apparent reaction kinetics is also maintained as can be observed in Fig. 16: the amine conversion is 64% at the reactor outlet whereas it is 65% at the same reaction time in batch conditions.

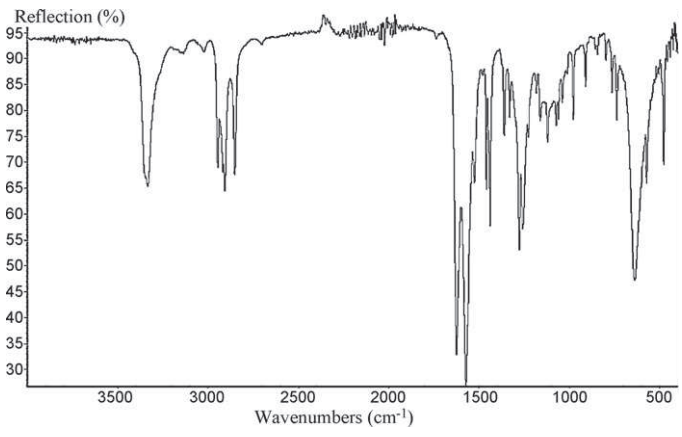

Fig. 13. FTIR spectra of polyurea obtained during experiment E1.

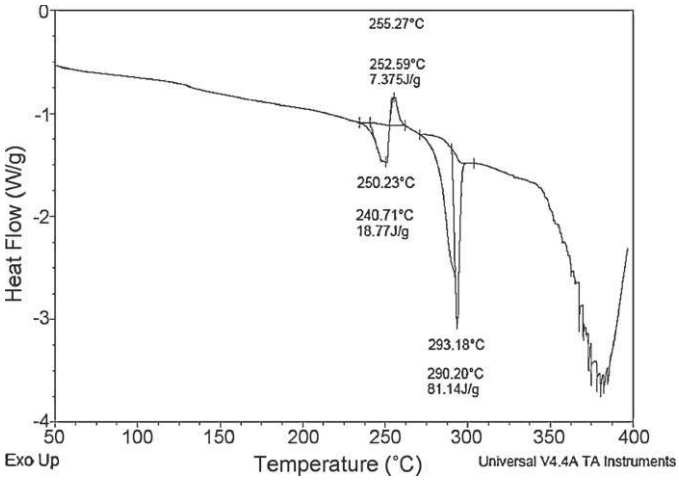

Fig. 14. DSC thermogram of polyurea obtained during the experiment E1.

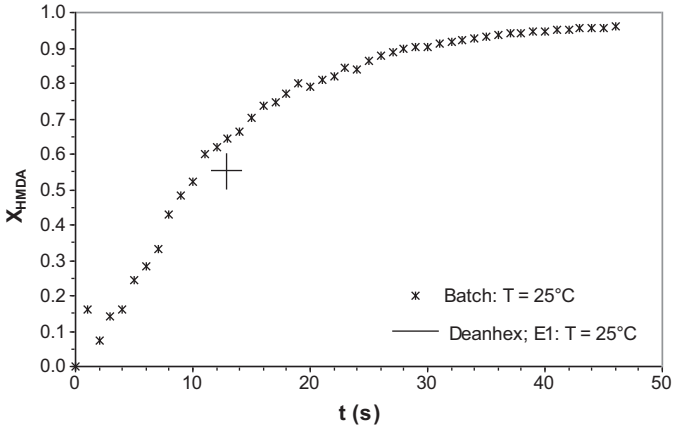

Fig. 15. Comparison between HMDA conversion at the Deanhex 2×2 outlet for experiment E1 to the batch data obtained in the same operating conditions: $T = 25\,^{\circ}C$, $C_{HMDA,0} = 4.1 \times 10^{-3}\,mol\,L^{-1}$, $Q_{tot} = 5.0\,L\,h^{-1}$, and $\Phi_{microcapsules} = 0.04$.

4.3.2. Influence of the temperature

There are only few studies investigating the influence of temperature on the reaction rate for microencapsulation by interfacial polycondensation batch processes. A reason could be that the reaction kinetics is fast enough at ambient temperature to be completed in a reasonably short time. In his review Arshady [42] mentioned that the reaction kinetics is influenced by the temperature of the polymerization mixture. Frere et al. [43] synthesized polyurethane microcapsules and showed that the reaction is accelerated when increasing the temperature. In a continuous process, the decrease of the reaction time will lead to a shorter reactor length potentially beneficial in terms of reactor compactness and investment costs.

Experiment E3 in the 2 mm width Deanhex reactor is carried out at 32 °C in order to evaluate the influence of the temperature on the apparent reaction kinetics. The 32 °C temperature is reached by heating the majority phase, i.e. the continuous phase containing HMDA, upstream from the reactor inlet. The HMDA conversion at reactor outlet is 90% whereas it is 64% at 25 °C. So a 7 °C increase in temperature results in a 30% increase in the HMDA conversion.

4.3.3. Influence of the reactor geometry

The flowrate in the 2 mm width Deanhex reactor is limited to about $15\,L\,h^{-1}$. In order to increase the microcapsules output it is possible to use a larger Deanhex. That is why the 4 mm width

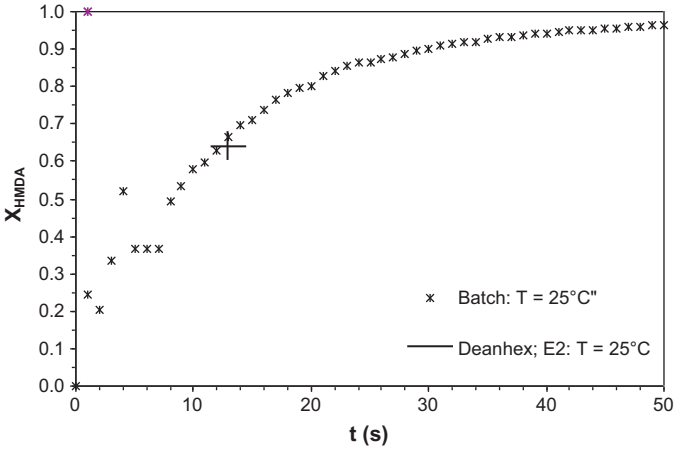

Fig. 16. Comparison between HMDA conversion at reactor outlet for experiment E2 to the batch data obtained in the same operating conditions: $T = 25\,^{\circ}C$, $C_{HMDA,0} = 7.7 \times 10^{-3}\,mol\,L^{-1}$, $Q_{tot} = 4.9\,L\,h^{-1}$, and $\Phi_{microcapsules} = 0.10$.

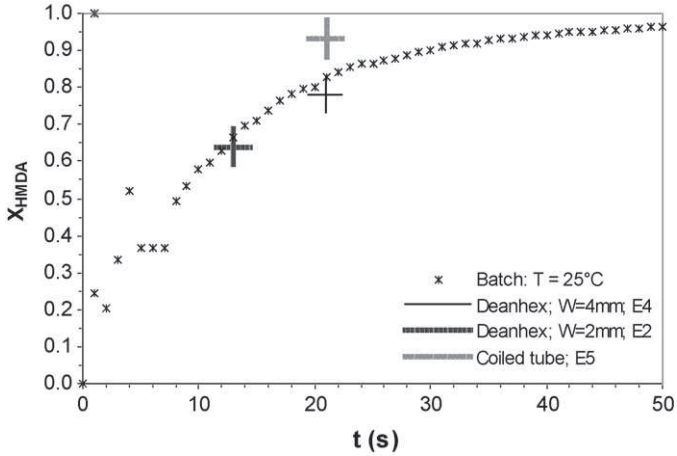

Fig. 17. Comparison between HMDA conversion at reactor outlet for experiments in the 4 mm width Deanhex reactor (E4), in the 2 mm width reactor (E2), and in the coiled tube reactor (E5), to batch data at $T = 25\,^{\circ}C$, and $\Phi_{microcapsules} \approx 0.10$.

Deanhex reactor is tested. Moreover it enables to perform the first step of a scale-up approach.

Working with one Deanhex reactor does not allow to complete the reaction as short residence times result from flowrates studied. The residence time may be increased by using several reactive plates in serial. But both Deanhex reactors remain interesting apparatuses in their one reactive plate configuration as they enable to study the first step of the reaction.

In order to easily increase the residence time to conduct such athermal reaction a classical coiled tube reactor can be also used.

Additional experiments are thus performed in the 4 mm width Deanhex reactor (experiment E4) and in a 50 m length coiled tube reactor (experiment E5). The diameter of this reactor is 4 mm and it is long enough to get 4 min residence time with a similar total flowrate than in the 4 mm Deanhex. This residence time does not allow to complete the reaction, but it is higher than the time corresponding to the occurrence of the agglomeration phenomenon (cf. Section 3.2.1). The HMDA conversion is calculated thanks to pH measurement at a reactor length (4.6 m) corresponding to a residence time of 21 s, similar to the residence time in the 4 mm Deanhex reactor. Let us note that the coiled tube reactor is not insulated, but the temperature is kept almost constant by controlling the HMDA solution stream temperature, fixed to 25 °C.

The HMDA conversion at the 4 mm width Deanhex reactor outlet is compared to the conversion obtained at the same reaction time in the coiled tube in Fig. 17. In this figure is also mentioned the HMDA conversion at the 2 mm width Deanhex reactor outlet.

The HMDA conversion at reactor outlet is 78% in the 4 mm width Deanhex reactor whereas it is 83% in batch conditions. This represents a 6% deviation that is rather satisfactory. The HMDA conversion follows the batch kinetics profile for both 2×2 and 4×4 Deanhex reactors. Increasing the hydraulic diameter of the Deanhex while keeping a similar Reynolds (≈700) number enables to increase both the residence time and the productivity, without any kinetics change.

The HMDA conversion after 21 s residence time in the coiled tube is about 93% whereas it is 83% in batch reactor for a same reaction time. The discrepancy may be explained by the pH measurement conditions. Nevertheless in spite of the pH measurement uncertainty this result indicates that the HMDA homogenization in continuous reactor is fast enough and consequently does not slow down the apparent reaction kinetics. The mixing conditions may thus be considered efficient enough regarding the reaction studied.

This kinetics study shows that the three continuous reactors tested allow to carry out the interfacial polycondensation reaction

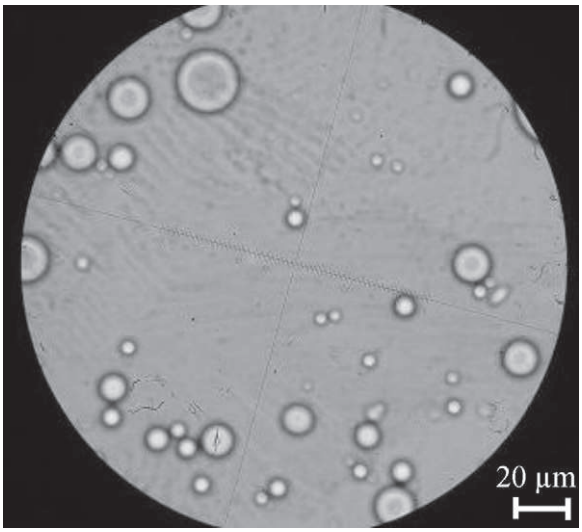

Fig. 18. Optical microscopy picture of emulsion's droplets obtained during experiment E1.

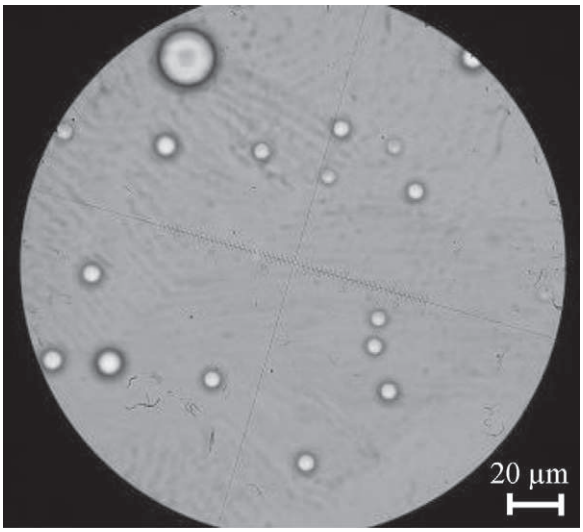

Fig. 19. Optical microscopy picture of microcapsules obtained during experiment E1.

without modifying the apparent reaction kinetics of the reaction performed in a classical stirred tank. Moreover the apparent reaction kinetics can be accelerated by increasing the working temperature.

4.4. Microcapsules size distributions

4.4.1. Comparison between emulsion droplets and microcapsules size distributions in dilute conditions

In order to assess the use of the continuous reactors for the whole continuous process, it is important to ensure that the emulsion droplets size distribution is not modified during the reaction. Experiment E1 is performed in dilute conditions ($\Phi_{microcapsules}$ = 5 vol.%), at T = 25 °C and with surfactant in the 2 mm width Deanhex reactor. Figs. 18 and 19 present optical microscopy pictures of emulsion droplets and microcapsules obtained during this experiment.

These pictures show that emulsion's droplets and microcapsules are spherical, and that microcapsules and emulsion's droplet sizes range are similar. Fig. 20 compares both emulsion and microcapsules size distributions obtained during this experiment.

Both distributions are similar and characterized by a log-normal profile. The Sauter mean diameters characterising these distributions are about 14 µm. These results indicate that neither droplets coalescence between the static mixer outlet and the reactor inlet nor microcapsules agglomeration in the reactor occur during this experiment. It is important to notice that the residence time in the 2 mm width channel reactor is about 10 s, what corresponds to a HMDA conversion at reactor outlet of 55%.

Thus no coalescence phenomenon occurs in the reactor until a conversion rate of 55% for a rather dilute system (5% in volume) and in presence of surfactant.

4.4.2. Increase of the microcapsules concentration

Experiments are carried out in the three reactors with a microcapsules concentration of 10% in volume (experiments E2 and E3 in the 2 mm width Deanhex reactor at respectively T = 25 °C and T = 32 °C, experiment E4 in the 4 mm width Deanhex reactor, and experiment E5 in the coiled tube reactor). At this concentration an agglomeration phenomenon has been highlighted in the stirred tank reactor (cf. Section 3.2.1)).

As shown in Fig. 21 the microcapsules size distribution at the 2 mm width Deanhex reactor outlet (experiment E2) that corresponds to about 10 s residence time, is similar to the emulsion droplets size one. At this concentration the hydrodynamic conditions in the 2 mm width Deanhex enable to carry out the encapsulation reaction without any aggregation or agglomeration phenomenon until a 64% HMDA conversion (experiment E2). The same observation is done at the outlet of the 4 mm width Deanhex reactor (experiment E4), where the residence time enables to reach 78% HMDA conversion.

The "critical" HMDA conversion at which the agglomeration phenomenon occurs is approached in the 2 mm width Deanhex reactor when increasing the temperature (experiment E3). In that case the HMDA conversion at reactor outlet is 90%, and no agglomeration phenomenon occurs.

The influence of the reactor hydrodynamic conditions on this agglomeration phenomenon is studied at a higher X_{HMDA} in the coiled tube (experiment E5), where the residence time is of 4 min at the tested flow rate. Several samples are taken along the reactor in order to observe the slurry behavior in the tube. The microcapsules size distributions corresponding to these samples are compared to the emulsion droplets size distribution at the static mixer exit in Fig. 22. Note that X_{HMDA} is higher than 95% at 115 s.

The whole distributions are monomodal and quite well superimposed. No agglomeration phenomenon is observed inside the

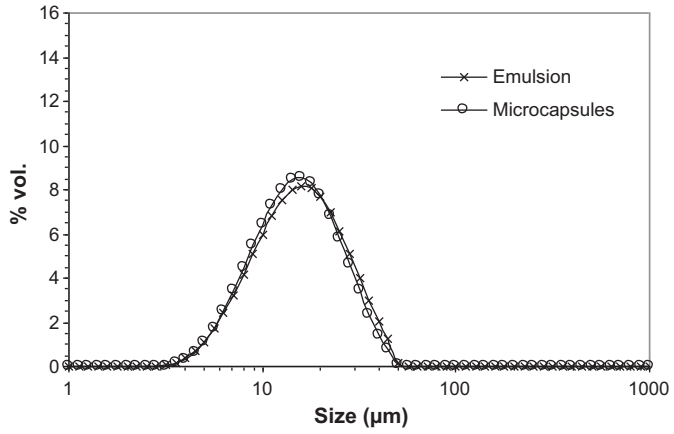

Fig. 20. Comparison between emulsion droplets and microcapsules size distributions for experiment E1 in the 2 mm width Deanhex reactor: T = 25 °C, $C_{HMDA,0} = 4.1 \times 10^{-3}$ mol L^{-1}, Q_{tot} = 5.0 L h^{-1}, and $\Phi_{microcapsules}$ = 0.04.

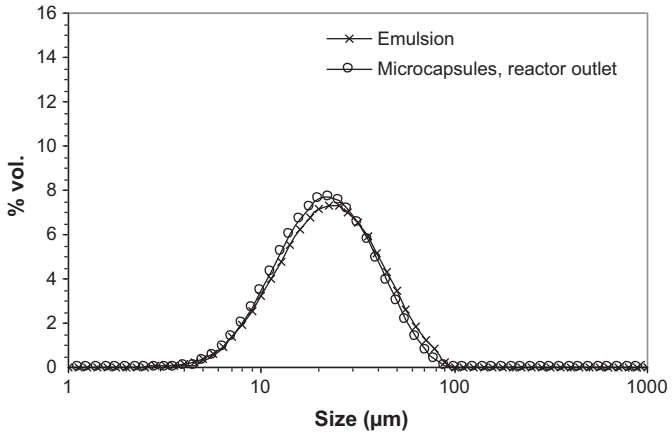

Fig. 21. Comparison between emulsion droplets and microcapsules size distributions for experiment E2 in the 2 mm width Deanhex reactor: $T = 25\,^{\circ}C$, $C_{HMDA,0} = 7.7 \times 10^{-3}$ mol L^{-1}, $Q_{tot} = 4.9$ L h^{-1}, and $\Phi_{microcapsules} = 0.10$.

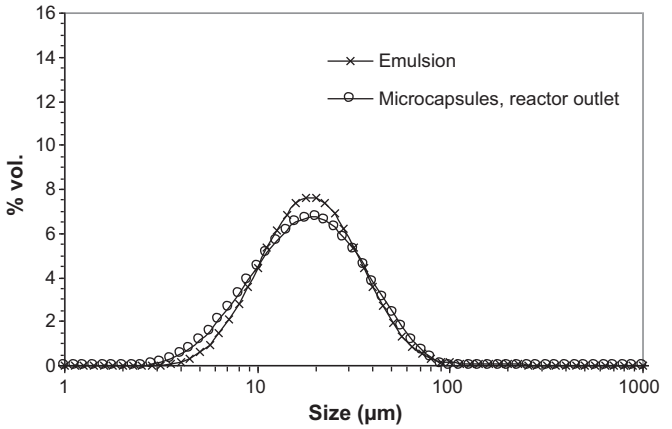

Fig. 23. Comparison between emulsion droplets and microcapsules size distributions obtained during experiment E3 in the 2 mm width Deanhex reactor: $T = 32\,^{\circ}C$, $C_{HMDA,0} = 7.7 \times 10^{-3}$ mol L^{-1}, $Q_{tot} = 5.2$ L h^{-1}, and $\Phi_{microcapsules} = 0.11$.

tube. Working continuously under favorable hydrodynamic conditions allows thus to avoid the agglomeration at this concentration.

To ensure that this agglomeration step well overcame, a sample of the slurry at reactor outlet is maintained under soft magnetic stirring during 24 h, in order to keep the microcapsules in suspension. After this time the reaction is considered to be completed. The microcapsules size distribution is then analyzed and compared to the distribution obtained just after sampling at the reactor outlet in Fig. 22.

The microcapsules size distribution after 24 h is quite well superimposed to the one at reactor outlet. The Sauter mean diameter of the former is 15 μm and is 13 μm for the latter. The discrepancy between both distributions is too small to reveal some phenomenon and is likely due to the measurement incertitude.

As a conclusion, the hydrodynamic conditions in such continuous reactors (coiled tube and Deanhex) allow to avoid the microcapsules agglomeration phenomenon for a 10% microcapsules concentration.

4.4.3. Influence of the temperature

It has not yet been demonstrated to what extend temperature could influence the polymer shell properties. Some microcapsules stuck fragments appearing when conducting the reaction at more than 45.5 °C are described by Frere et al. [43], but there is little information available in the literature about eventual modifications of microcapsules structure when increasing the reaction temperature.

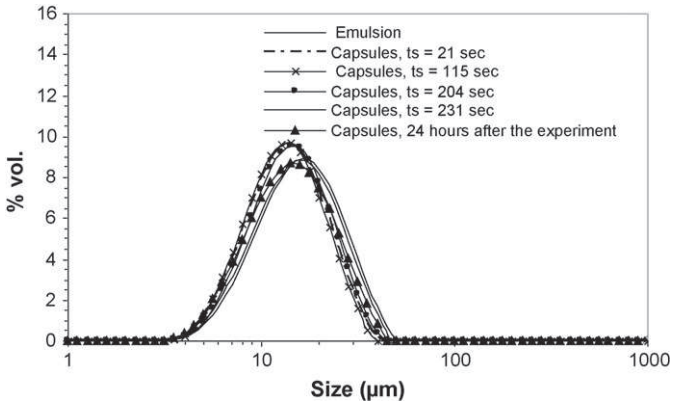

Fig. 22. Comparison between emulsion droplets and microcapsules size distributions at different coiled tube positions and 24 h after the experiment for experiment E5: $T = 25\,^{\circ}C$, $C_{HMDA,0} = 7.7.10^{-3}$ mol L^{-1}, $Q_{tot} = 9.8$ L h^{-1}, and $\Phi_{microcapsules} = 0.10$.

As described in Section 4.4.2, the reaction kinetics is accelerated by a temperature increase. The experiment E3 enables to test whether the droplets size distribution is modified during encapsulation when operating at 32 °C. Fig. 23 shows that at this temperature the microcapsules size distribution is quite superimposed to the emulsion droplets one.

4.4.4. Experiments without surfactant

In microencapsulation by interfacial polycondensation processes, surfactants are generally used for their ability to reduce the droplets sizes [44–46] and to prevent them from coalescence [45,47]. If the size reducing property is necessary depending on the microcapsules characteristics required, the stabilizing effect is needed when typical stirred tank processes are involved. In fact surfactants are used in order to prevent from coalescence involved in stirred tank emulsification process, and eventually at the beginning of the reaction when the second monomer is added in the continuous phase. During the reaction, it is assumed that the polymer membrane hardens the interface [13,15,38].

During the emulsification step of the continuous process studied, the hydrodynamic conditions in the static mixer result in low coalescence probability. Subsequently, the second monomer is quickly added at the mixer outlet, which allows to stiffen the interface over a significantly reduced time period. As a matter of fact, a monomodal microcapsules size distribution might be expected to be obtained even though no surfactant is added.

Experiment E6 is performed without surfactant at low microcapsules concentration of about 5% in volume in order to avoid the agglomeration of microcapsules. Moreover the recirculation flowrate inside the static mixer is fixed to about 335 L h^{-1} in order to reach emulsion droplet sizes low enough to guarantee a minimum stability before encapsulation. This experiment without surfactant is performed in the coiled tube reactor at 25 °C in order to reach almost 100% HMDA conversion.

No agglomeration phenomenon is noticeable inside the reactor, and the microcapsules size distribution at reactor outlet presented in Fig. 24 shows a monomodal profile with a Sauter mean diameter of 45 μm and a maximum diameter of about 110 μm. As expected these characteristic diameters are quite higher than those obtained with surfactant.

The HMDA conversion at the first sampling point corresponding to a residence time of 20 s is of 83% whereas it was of about 95% at the same time in batch conditions. This 13% deviation might be explained not only by the incertitude due to the pH measurement method, but also by a decrease of the apparent reaction rate. In fact, higher microcapsules sizes result in a lower interfacial area

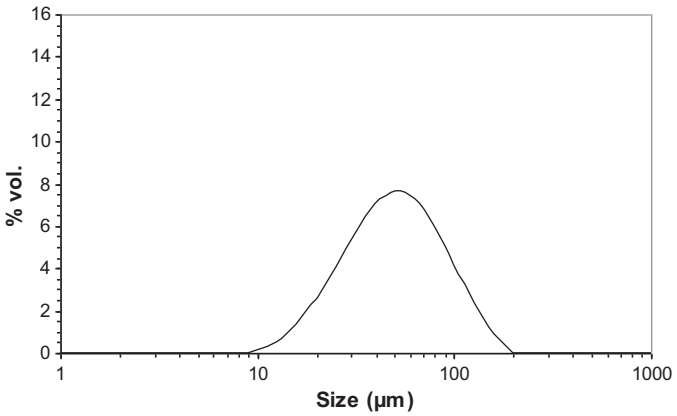

Fig. 24. Microcapsules size distribution obtained during experiment E6 without surfactant in the coiled tube: $T = 25\,^{\circ}C$, $C_{HMDA,0} = 4.7 \times 10^{-3}$ mol L^{-1}, $Q_{tot} = 10.0$ L h^{-1}, and $\Phi_{microcapsules} = 0.06$.

between both phases what may result in a decrease of the reaction rate.

5. Conclusion

This study shows a stepped-approach to transfer a classical batch process to a continuous one. Such an approach needs prior considerations to detect the main issues of the original process in order to select the most appropriate continuous technical device for each step. Concerning microcapsules obtained by interfacial polycondensation, if the influence of formulation on end use properties is widely commented in the literature, only few studies deal with the process influence on the reaction performances. Therefore if microcapsules end use properties seem to depend only on formulation, this paper highlights that their size control as well as the production yield can be improved significantly through a better process control.

The association of two continuous apparatuses proposed enables to well control the microcapsules size obtained. The first step, performed in static mixer, allows to generate the emulsion with targeted droplets size. The second step, carried out in continuous reactors with appropriate hydrodynamic conditions, allows to complete the reaction without agglomeration phenomenon.

The PMMA Deanhex reactor enables to observe the microcapsules behavior during the first seconds of the reaction. To carry out the reaction until its end, the classical coiled-tube reactor is used. In both continuous reactors the reaction apparent kinetics is in good agreement with semi-batch results.

The continuous microencapsulation process proposed here offers interesting ways of intensification. Indeed the use of both continuous reactors tested enables to limit process losses due to the agglomeration phenomenon when increasing the microcapsules concentration. Moreover this continuous process allows the increase of the process yield through the increase of microcapsules concentration and the ability to work without surfactant. This last result is really interesting as it enables to avoid typical issues of post-treatments due to the presence of the surfactant and it may offers the possibility to better control the microcapsules membrane properties.

Finally the use of the Deanhex reactor for the reaction step offers interesting outlooks for exothermic inhomogeneous reactions involving liquid–liquid systems. In fact, it has been demonstrated that the hydrodynamic conditions in such intensified apparatus enable to ensure the droplets size distribution obtained during the emulsification step is not changed during the reaction. On this basis the availability of the Deanhex reactor to carry out safely exothermic reactions could be exploited for cases of heterogeneous liquid–liquid reactions.

References

[1] P.W. Morgan, S.L. Kwolek, Interfacial polycondensation. Fundamentals of polymer formation at liquid interfaces, J. Pol. Sci. 40 (1959) 299–327.
[2] E.L. Wittbecker, P.W. Morgan, Interfacial polycondensation I, J. Pol. Sci. 40 (1959) 289–297.
[3] P.B. Deasy, Microencapsulation and related drug processes, Marcel Dekker, New York, 1984.
[4] A. Kondo, Microcapsule Processing and Technology, Marcel Dekker, New York, USA, 1979.
[5] G.H. Desai, K.H. Jin Park, Recent developments in microencapsulation of food ingredients, Drying Technol. 23 (2005) 1361–1394.
[6] A. Madene, M. Jacquot, J. Scher, S. Desobry, Flavor encapsulation and controlled release—a review, Int. J. Food Sci. Technol. 41 (2006) 1–21.
[7] G. Nelson, Application of microencapsulation in textiles, Int. J. Pharm. 242 (2002) 55–62.
[8] K.Y. Choi, K.S. Min, T. Chang, Microencapsulation of pesticides by interfacial polymerization: 2. Polyamide microcapsules containing water soluble-drug, Polymer (Korea) 15 (1991) 548–555.
[9] F. Puel, S. Briançon, H. Fessi, Industrial technologies and scale-up, in: Microencapsulation: Methods and Industrial applications, 2nd ed., Taylor and Francis Group, London, 2006, 149–182.
[10] P. Siddhan, M. Jassal, A.K. Agrawal, Core content and stability of *n*-octadecane-containing polyurea microcapsules produced by interfacial polymerization, J. Appl. Pol. Sci. 106 (2007) 786–792.
[11] F. Theron, N. Le Sauze, A. Ricard, Turbulent liquid–liquid dispersion in Sulzer SMX mixer, Ind. Eng. Chem. Res. 49 (2010) 623–632.
[12] F.A. Streiff, P. Mathys, T.U. Fischer, New fundamentals for liquid–liquid dispersion using static mixers, Récents Progrès en Génie des Procédés 11 (1997) 307–314.
[13] J. Legrand, P. Morançais, G. Carnelle, Liquid–liquid dispersion in an SMX-Sulzer static mixer, Trans. IChemE 79 (2001) 949–956.
[14] R.K. Thakur, C. Vial, K.D.P. Nigam, E.B. Nauman, G. Djelveh, Static mixers in the process industry—a review, Trans. IChemE 81 (2003) 787–826.
[15] P.K. Das, J. Legrand, P. Morançais, G. Carnelle, Drop breakage model in static mixers at low and intermediate Reynolds number, Chem. Eng. Sci. 60 (2005) 231–238.
[16] A.M. Al Taweel, L.D. Walker, Liquid dispersion in static in-line mixers, Can. J. Chem. Eng. 61 (1983) 527–533.
[17] A.M. El Hamouz, A.C. Stewart, G.A. Davies, Kerosene/water dispersions produced by a Lightnin in-line static mixer, IChemE Sym. Ser. 136 (1994) 457–464.
[18] Z. Anxionnaz, M. Cabassud, C. Gourdon, P. Tochon, Heat exchanger/reactors (HEX reactors): concepts, technologies: state-of-the-art, Chem. Eng. Process. 47 (2008) 2029–2050.
[19] Z. Anxionnaz, M. Cabassud, C. Gourdon, P. Tochon, Transposition of an exothermic reaction from a batch reactor to an intensified one, Heat Transfer Eng. 31 (2010) 788–797.
[20] W. Benaissa, N. Gabas, M. Cabassud, D. Carson, S. Elgue, M. Demissy, Evaluation of an intensified continuous heat-exchanger reactor for inherently safer characteristics, J. Loss Prev. Process Ind. 21 (2008) 528–536.
[21] S. Ferrouillat, P. Tochon, D. Della Valle, H. Peerhossaini, Open loop thermal control of exothermal chemical reactions in multifunctional heat exchangers, Int. J. Heat Mass Transfer 49 (2006) 2479–2490.
[22] Z. Anxionnaz, M. Cabassud, C. Gourdon, P. Tochon, Hydrodynamic study and optimization of the geometry of a wavy channel in an intensified heat exchanger/reactor, in: 2nd GPE-EPIC, Venice (Italy), 2009, pp. 14–17.
[23] D.M. Ruthven, The residence time distribution for ideal laminar flow in a helical tube, Chem. Eng. Sci. 26 (1971) 1113–1121.
[24] R.N. Trivedi, K. Vasudeva, RTD for diffusion free laminar flow in helical coils, Chem. Eng. Sci. 29 (1974) 2291–2295.
[25] R.N. Trivedi, K. Vasudeva, Axial dispersion in laminar flow in helical coils, Chem. Eng. Sci. 30 (1975) 317–325.
[26] E.B. Nauman, The residence time distribution for laminar flow in helically coiled tubes, Chem. Eng. Sci. 32 (1977) 287–293.
[27] S.K. Yadav, A.K. Suresh, K.C. Khilar, Microencapsulation in polyurea shell by interfacial polycondensation, AIChE J. 36 (1990) 431–438.
[28] S.K. Yadav, K.C. Khilar, A.K. Suresh, Microencapsulation in polyurea shell: kinetics and film structure, AIChE J. 42 (1996) 2616–2626.
[29] S.S. Dhumal, S.J. Wagh, A.K. Suresh, Interfacial polycondensation—modelling of kinetics and film properties, J. Membr. Sci. 325 (2008) 758–771.
[30] S.S. Dhumal, A.K. Suresh, Understanding interfacial polycondensation: experiments on polyurea system and comparison with theory, Polymer 51 (2010) 1176–1190.
[31] S.J. Wagh, S.S. Dhumal, A.K. Suresh, An experimental study of polyurea membrane formation by interfacial polycondensation, J. Membr. Sci. 328 (2009) 246–256.
[32] L.J.J.M. Janssen, K. Te Nijenhuis, Encapsulation by interfacial polycondensation, I. The capsule production and a model for wall growth, J. Membr. Sci. 65 (1992) 59–68.
[33] L.J.J.M. Janssen, K. Te Nijenhuis, Encapsulation by interfacial polycondensation, II. The membrane wall structure and the rate of the wall growth, J. Membr. Sci. 65 (1992) 69–75.

[34] J. Ji, B.J. Trushinski, R.F. Childs, J.M. Dickson, B.E. Mccarry, Fabrication of thin-film composite membranes with pendant, photoreactive diazoketone functionality, J. Appl. Pol. Sci. 64 (1996) 2381– 2398.
[35] S.K. Karode, S.S. Kulkarni, A.K. Suresh, R.A. Mashelkar, New insights into kinetics and thermodynamics on interfacial polymerization, Chem. Eng. Sci. 53 (1998) 2649–2663.
[36] S.K. Yadav, N. Ron, D. Chandrasekharam, K.C. Khilar, A.K. Suresh, Polyureas by interfacial polycondensation: preparation and properties, J. Macromol. Sci.: Phys. B35 (1996) 807–827.
[37] M. Kubo, Y. Harada, T. Kawakatsu, T. Yonemoto, Modelling of the formation kinetics of polyurea microcapsules with size distribution by interfacial polycondensation, J. Chem. Eng. Japan 34 (2001) 1506–1515.
[38] K. Hirech, S. Payan, G. Carnelle, L. Brujes, J. Legrand, Microencapsulation of an insecticide by interfacial polymerisation, Powder Technol. 130 (2003) 324–330.
[39] Z. Anxionnaz, M. Cabassud, C. Gourdon, P. Tochon, Thermo-hydraulic study and optimization of the wavy channel geometry of an intensified heat exchanger/reactor, Récents Progrès en Génie des Procédés 98 (2009).
[40] O. Levenspiel, Chemical Reaction Engineering, 3rd ed., John Wiley & Sons, New York, 1999, 90–119.
[41] H. Fellouah, C. Castelain, A. Ould El Moctar, H. Peerhossaini, A criterion for detection of the onset of Dean instability in Newtonian fluids, Eur. J. Mech. B/Fluids 25 (2006) 505–531.
[42] R. Arshady, Review preparation of microspheres and microcapsules by interfacial polycondensation techniques, J. Microencapsul. 6 (1989) 13–28.
[43] Y. Frere, L. Danicher, P. Gramain, Preparation of polyurethane microcapsules by interfacial polycondensation, Eur. Pol. J. 88 (1998) 1162–1169.
[44] D.Y. Chao, The role of surfactants in synthesizing polyurea microcapsule, J. Appl. Pol. Sci. 47 (1993) 645–651.
[45] N. Yan, P. Ni, M. Zhang, Preparation and properties of polyurea microcapsules with non-ionic surfactant as emulsifier, J. Microencapsul. 10 (1993) 375–383.
[46] Y.M. Kuo, C.T. Wu, W.H. Wu, D.Y. Chao, Effect of surfactants on the particle sizes of red 170 polyurea microcapsules, J. Appl. Pol. Sci. 52 (1994) 1165–1173.
[47] M. Zhang, P. Ni, N. Yan, Effect of operation variables and monomers on the properties of polyamide microcapsules, J. Microencapsul. 12 (1995) 425–435.